Langmuir

ARTICLE

pubs.acs.org/Langmuir

Polydiacetylene Incorporated with Peptide Receptors for the Detection of Trinitrotoluene Explosives

Justyn Jaworski,[†,‡,§] Keisuke Yokoyama,[∥] Chris Zueger,[⊥] Woo-Jae Chung,[‡,#] Seung-Wuk Lee,[*,‡,§,#] and Arun Majumdar[▽]

[†]Joint Graduate Group in Bioengineering, University of California, Berkeley, California 94720 and University of California, San Francisco, California 94143, United States

[‡]Department of Bioengineering, University of California, Berkeley, California 94720, United States

[⊥]Department of Mechanical Engineering, University of California, Berkeley, California 94720, United States

[§]Berkeley Nanoscience and Nanoengineering Institute, Berkeley, California 94720, United States

[∥]NSK Ltd., Tokyo, Japan

[#]Physical Biosciences Divisions, Lawrence Berkeley National Laboratory, Berkeley, California 94720, United States

[▽]ARPA-E, United States Department of Energy, Washington, D.C. 20585, United States

Supporting Information

ABSTRACT: Because of their unique optical and stimuli-response properties, polydiacetylene-based platforms have been explored as an alternative to complex mechanical and electrical sensing systems. We linked chromic responsive polydiacetylene (PDA) onto a peptide-based molecular recognition element for trinitrotoluene (TNT) molecules in order to provide a system capable of responding to the presence of a TNT target. We first identified the trimer peptide receptor that could induce chromic changes on a PDA backbone. We then investigated the multivalent interactions between TNT and our peptide-based receptor by nuclear magnetic resonance (NMR) spectroscopy. We further characterized various parameters that affected the conjugated PDA system and hence the chromic response, including the size of end-group motifs, the surface density of receptors, and the length of alkane side chains. Taking these necessary design parameters into account, we demonstrated a modular system capable of transducing small-molecule TNT binding into a detectable signal. Our conjugated PDA-based sensor coupled with molecular recognition elements has already proven useful recently in the development of another sensitive and selective electronic sensor, though we expect that our results will also be valuable in the design of colorimetric sensors for small-molecule detection.

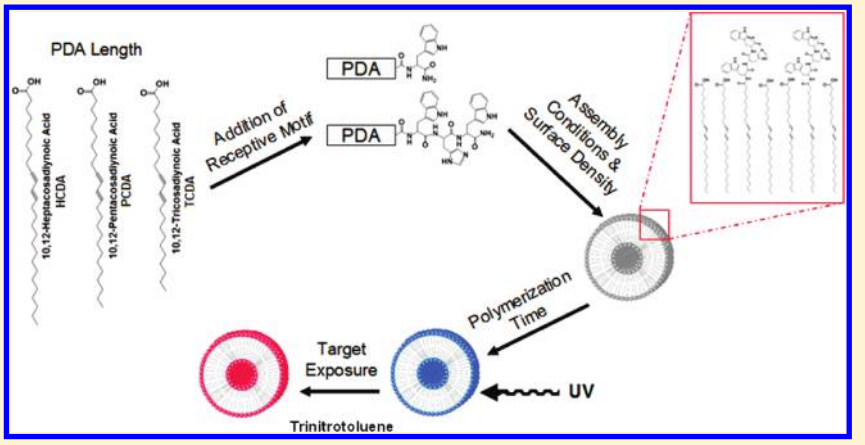

1. INTRODUCTION

Our environment contains a vast assortment of chemical and biological information, some of which we can perceive through our senses. For instance, our olfaction and gustation systems provide us with a means of molecular identification through smells and tastes. Unfortunately, many surrounding harmful biological and chemical species, which may threaten our health, remain undetectable. As such, we rely on the ability of sensor technologies to identify the hidden information in our environment. As an alternative to complex electromechanical sensing platforms, researchers have explored the use of molecular target interactions and subsequent transduction into a detectable color change as a means of gaining environmental information. One such colorimetric-based sensor framework utilizes the ability of inorganic nanoparticles to possess different absorption spectra depending on their interparticle spacing (or aggregation). Several research groups have demonstrated this with noble metal nanoparticles[1−7] and other inorganic nanostructures including

Received: November 9, 2010
Revised: January 6, 2011

   dx.doi.org/10.1021/la104476p | *Langmuir* XXXX, XXX, 000–000

quantum dots.[8−10] When incorporated with molecular recognition elements, these nanoparticles are effective sensing systems capable of a visible color change. Other colorimetric-based sensing approaches have minimized the need for signal transduction hardware by using receptors designed for specific molecular recognition that may elicit large spectral shifts upon ligand binding. Such systems make use of engineering the curvature and functionality of the receptor to provide the shape, size, and binding modes complementary to a given target molecule. These include cavitands, crown ethers, and metalloporphyrin dyes that can provide a visually detectable color change depending on the particular target−receptor pair.[11−13] Researchers have also utilized chromically responsive polymers functionalized with recognition sites for sensing purposes.[14−20] In this work, we examine the design parameters involved in the creation of chemical/biological sensors that utilize peptide-based recognition elements functionalized to such chromically responsive conjugated polymer systems.

Several groups have exploited π-conjugated polymers, particularly polydiacetylenes (PDAs), for chemical sensing applications because of the ability of their absorption spectra to change in response to target binding.[17−19,21−25] PDA is an amphiphilic polymer composed of a carboxylic acid head group and an alkyl tail that facilitates its formation into supramolecular assemblies.[26,27] When these assemblies are exposed to UV irradiation, a conjugated PDA (ene−yne) carbon backbone is formed that exhibits strong absorbance peaks at 640 or 540 nm resulting in a blue or red color, respectively.[28] The existence of a blue or red state is very dependent on the extent of planarity or π-orbital overlap of the conjugated PDA backbone.[28−30] PDA has been used extensively because of this susceptibility of the absorption spectrum to be altered by the shortening of the effective conjugation length resulting from external stimuli.[31−35] External stimuli, including interfacial perturbations or binding, can induce strain and distortions within side chains of PDA resulting in conformational transitions in the backbone.[36] This transition breaks the conjugated backbone network planarity resulting in increased absorption at lower wavelengths and hence a red chromatic transition.[37,38] Molecular interactions resulting in the disturbance of interfacial hydrogen bonds have been proven to create a stress on the polymer backbone sufficient to affect the polymers' conjugations length.[39−42] This change in the effective conjugation length of the π-conjugated backbone can be observed directly through the PDA absorption spectra, thereby making it ideal for sensing purposes.[35,43] Only a few degrees of (ene−yne) C−C bond rotation can cause the irreversible chromic shift to the red state.[28] The side-chain arrangement is therefore critical to the chromic response of the system, as we investigate below. In this work, we study the design parameters that affect the functionality of these conjugated polymer systems in colorimetric sensing applications for the detection of predetermined targets.

Using a modular synthesis strategy, we created sensors comprising a TNT recognition motif, identified previously through phage display,[44] coupled to chromic responsive PDA elements. By observing the absorption spectra changes of this system, we first determined the peptide-based molecular recognition elements that were effective in signal transduction from the TNT binding event into the colorimetric change. We then analyzed the possible binding mode of the TNT target molecule to the peptide recognition elements using nuclear magnetic resonance spectroscopy. Furthermore, we investigated the role of side-chain composition and surface density on self-assembly as well as the transduction of surface interactions to the conjugated PDA backbone. By investigating these assembly parameters, we have demonstrated the importance of polymerization timescales in achieving maximal effective backbone conjugation. The irreversible nature of the chromatic transition, from a metastable blue phase to a more thermodynamically stable red phase, was also explored through polymerization and heating experiments.[38] These parameters that we have established are critical considerations for PDA-based sensor fabrication.

2. MATERIALS AND METHODS

PDA−Peptide Conjugate Synthesis. To produce PDA−peptide conjugates, standard solid-phase peptide synthesis was carried out using Fmoc chemistry.[45] Fmoc-protected amino acids and rink amide resins were obtained from EMD Biosciences (San Diego, CA), and 10,12-pentacosadiynoic acid (PCDA) was obtained from Sigma-Aldrich (St. Louis, MO). Resins were preswelled for 30 min in NMP prior to deprotection. Deprotection steps using 3 mL of 3% DBU in NMP were carried out for 20 min on a rocking platform. The washing steps proceeded as follows: three washes with 4 mL of NMP, six washes with the series of 4 mL of methanol followed by 4 mL of dichloromethane, and three washes with 4 mL of NMP. Coupling steps of 3 mL and 0.2 M amino acid, Hobt, and DIC were carried out on a rocking platform for 2 h. A final coupling step with 3 mL of 0.2 M 10,12-pentacosadiynoic acid (PCDA), Hobt, and DIC was performed with the same incubation period of 2 h to create the PCDA−peptide conjugate. PCDA was replaced with (TCDA) 10,12-tricosadiynoic acid, (HCDA), 10,12-heptacosadiynoic acid, (HDA) 4,6-heptadiynoic acid, or (NDA) 6,8-nonadiynoic acid to create additional systems for analyzing the chain-length parameters. For NMR samples lacking an alkane chain, the short peptides did not undergo this final conjugation step. Kaiser tests were performed at each step to identify the presence of primary amines in order to monitor the extent of reaction.[46] Resins were washed with methylene chloride and dried and then underwent cleavage. Cleavage reactions were performed for 2 h while shaking with a cocktail of 82.5% trifluoroacetic acid, 5% water, 5% phenol, 5% ethanedithiol, and 2.5% triisopropylsilane. Rotary evaporation followed by precipitation in diethyl ether provided the removal of cleavage solvents and protecting groups. Samples were then suspended and mixed in water, followed by centrifugation for 10 min at 10 000 rpm to pellet the product, at which point the supernatant was discarded to remove any trace contaminants. The suspension and centrifugation steps were repeated until all cleavage contaminants were removed. Lyophilization was then performed, and samples were stored at 4 °C. The PDA−peptide conjugates, which were synthesized, are as follows: PCDA-Trp-His-Trp (TNT binding motif), TCDA-Trp-His-Trp, HCDA- Trp-His-Trp, HDA-Trp-His-Trp, and NDA-Trp-His-Trp.

Size Characterization. Fully polymerized supramolecular assemblies with 4% PCDA-Trp-His-Trp and 96% PCDA were deposited on a polished silicon prime wafer and imaged using atomic force microscopy (MFP-3D, Asylum Research, Santa Barbara, CA). AFM image traces were used to build a histogram that revealed an average diameter of between 150 and 200 nm. Additionally, dynamic light scattering confirmed an average monomodal hydrodynamic diameter of 162 nm indicating a single size distribution (Figure S2 in the Supporting Information)

Controlling the Surface Composition and Density in Supramolecular Assemblies. PCDA and PCDA−peptide conjugates were suspended to 10 mM in water. Solutions were sonicated for 20 min and held at 85 °C for 20 min to melt any existing supramolecular structure. Additional sonication for 20 min was performed prior to the mixing of PCDA with PCDA−peptide conjugates. Volumetric mixing was utilized to provide the exact molar amount of PCDA and peptide conjugate. For example, 4% PCDA-Trp-His-Trp and 96% PCDA utilized a 4:96 volumetric ratio of PCDA-Trp-His-Trp to PCDA. After

dx.doi.org/10.1021/la104476p |Langmuir XXXX, XXX, 000–000

mixing, the sample was heated for another 5 min at 85 °C and sonicated to ensure an ample distribution of PCDA−peptide conjugates and PCDA. To allow self-assembly, the solution was allowed to cool to room temperature and then incubated at 4 °C for 24 h. The solution was then brought to room temperature, and the supramolecular self-assemblies were polymerized using a 4 W UV lamp at a wavelength of 254 nm. Polymerization was carried out for 25 min of exposure. After the polymers were filtered through a 0.8 μm cellulose acetate filter, the size was measured using a dynamic light scattering (DLS) particle sizer (Malvern Instruments, Southborough, MA).

UV Exposure, Extent of Polymerization, and Irreversibility Measurements. The extent of PCDA polymerization was characterized from the visible absorption spectra (400−800 nm wavelength scan with a Beckman Coulter UV−visible spectrophotometer). In particular, the blue percentage, $[Abs_{640}/(Abs_{640}+ Abs_{540})] \times 100\%$, and the chromic response, [(initial blue percentage − exposed blue percentage)/initial blue percentage] × 100%, were used to characterize the polymerization parameter of the conjugated π backbone. To identify the irreversibility of the system and the timescale on which UV polymerization is complete, a 10 mM solution of PCDA, prepared as described above, was initially polymerized by exposure to 5 min of UV light (4 W lamp at 254 nm). The resulting spectrum was obtained, and the blue percentage was determined. The solution was then exposed to 70 °C for 5 min to thermally induce a chromatic transition to the red phase, at which point the blue percentage color was again obtained through spectral analysis. This process was repeated until the blue percentage remained constant, indicating complete polymerization and the irreversibility of the system.

To confirm the polymerization time necessary to achieve the greatest potential chromic response, freshly prepared PCDA samples were exposed to UV light for periods of 5 s, 10 s, 30 s, 1 min, 2.5 min, 5 min, 7.5 min, 10 min, 15 min, 20 min, or 25 min. The blue percentage was calculated from the obtained spectra, and the solutions were then exposed to a thermal stimulus of 70 °C overnight to induce a complete chromatic transition. From the resulting spectra, the exposed blue percentage was obtained to calculate the chromic response. The necessary polymerization conditions for maximal chromic response could then be determined.

NMR Experiments of TNT Association with Peptide Motifs. As mentioned above, the short peptides for NMR experiments were created using solid-phase peptide synthesis to provide pure forms of the active motif for NMR spectroscopy. Rink amide resin was used for the 0.7 mmol scale synthesis of Trp-His-Trp, Ala-His-Trp, and Trp-His-Ala. Samples were purified by HPLC to >97% purity. Target solutions were prepared as follows. Trinitrotoluene targets were prepared in D_2O solutions at 0.57 mM. Peptides samples were dissolved in TNT solution at receptor concentrations of 0 to 50 mM. ^{1}H NMR spectra were recorded on a Bruker AVQ-400 (400 MHz) Fourier transform NMR spectrometer at the University of California, Berkeley, NMR facility. ^{1}H NMR resonances were reported in units of ppm downfield from tetramethylsilane assigned to zero because tetramethylsilane was used as the internal standard for ^{1}H NMR spectra determined in D_2O solvent.

Identifying the Role of Trp in the TNT Binding Motif, Trp-His-Trp. Using the chemical shifts observed (Δ_{obs}) from the titration data from varying concentrations of peptide, the Benesi−Hildebrand equation could be used, $1/\Delta_{obs} = 1/([\text{peptide}]K_a\Delta_{max}) + 1/\Delta_{max}$. By plotting the inverse of Δ_{obs} on the y axis and the inverse of the peptide concentration on the x axis, the binding constant, K_a, could be determined from the slope and intercept. The values of the association constants obtained for various peptide motifs demonstrate the relatively small role of the methyl group interaction in the recognition event as compared to that of the aromatic group of TNT. Interestingly, we see that the contribution to methyl binding maintains the same trend across the various peptide motifs whereas the aromatic interactions change dramatically from the Trp-His-Trp to Trp-His-Ala case. This contribution of the different side chains in the molecular interactions taking place with the TNT molecule seems to decrease when the dual aromatic residue motif is disrupted by the replacement of the Trp with an Ala or similarly for monomeric Trp.

Altering the Surface Density. PCDA mixtures containing 0, 4, 8, 14, 25, 30, 50, and 100% PCDA-Trp-His-Trp surface density were prepared as described above. Importantly, all samples were prepared from the same initial stock solutions in order to minimize variation in the spectral response. The samples were UV polymerized for 25 min, and the resulting blue percentage was measured to identify the effect of surface density on assembling into a planar conjugated system; thereby, the propensity for steric-induced red-phase transitions was examined.

Varying the Alkane Side-Chain Length. In addition to the PCDA-Trp-His-Trp motif, several other PDA constructs with varying alkane side-chain lengths were produced that possessed the same TNT binding motif. This was carried out by using the same synthesis protocol as listed above but replacing the PCDA component with HCDA, TCDA, HDA, or NDA. To identify the effect of chain length, TCDA-Trp-His-Trp-, HCDA-Trp-His-Trp-, and PCDA-Trp-His-Trp-based assemblies were created using the same protocol as listed above with compositions containing a 10% surface density of peptide (10% molar ratio of PDA-Trp-His-Trp in PDA). Samples were prepared in 200 μL aliquots within a 96-well clear-bottom plate for the analysis of the absorbance spectra using a Safire2 plate reader (TECAN, Männedorf, Switzerland). The plate was shaken for 2 s prior to sample measurement, and each sample was subjected to 10 readings, at which point the absorbance was averaged. Samples were then subjected to TNT at concentrations of 5.2, 9.5, 20.3, and 33.6 μM. Again, the absorbance spectra were obtained after TNT exposure using the Safire2 plate reader. The resulting chromic response to TNT exposure was calculated from the blue percentage of TNT exposure aliquots in relation to no TNT exposure aliquots as described above. Additional analysis of the sensitivity effect on the length between the head group and the polydiacetylene backbone was carried out as above with (HDA) 4,6-heptadiynoic acid and (NDA) 6,8-nonadiynoic acid at a composition of 5% surface density of peptide.

3. RESULTS AND DISCUSSION

Determination of the Essential Peptide-Based Molecular Recognition Elements on PDA. We first determined the essential TNT recognition elements from UV−vis spectroscopy for PDA sensor unit fabrication. We first synthesized full-length TNT binding peptides (Trp-His-Trp-Gln-Arg-Pro-Leu-Met-Pro-Val-Ser-Ilu) previously reported[44] to be coupled with PCDA chains. However, the resulting TNT receptor−PDA construct did not exhibit any colorimetric change for TNT addition (Data not shown). The truncated version, Trp-His-Trp-Gln-PDA, was also not sensitive. This implies that the distance between the binding site and PDA backbone is too great to induce any electronic band change in the PDA. We began to observe the colorimetric responses from the trimer peptide (Trp-His-Trp) in response to the TNT target by way of the (Trp-His-Trp)-coupled PDA (PCDA). When Trp-His-Trp-PDA was suspended in DI water, it formed stable vesicles with a size distribution of 150−200 nm as observed by AFM (Figure S1). Dynamic light scattering confirmed that the average diameter of vesicle is 162 nm (Figure 2a). We confirmed the efficacy of the receptor while attached to PDA by observing the binding ability between the recognition element (Trp-His-Trp) and TNT to alter the electronic band structure of the PDA conjugated backbones. We analyzed this signal transduction event directly by observing changes in UV−vis spectra upon mixing TNT with PDA-Trp-His-Trp assemblies (Figure 2b). The addition of an 11 μM TNT

dx.doi.org/10.1021/la104476p |Langmuir XXXX, XXX, 000–000

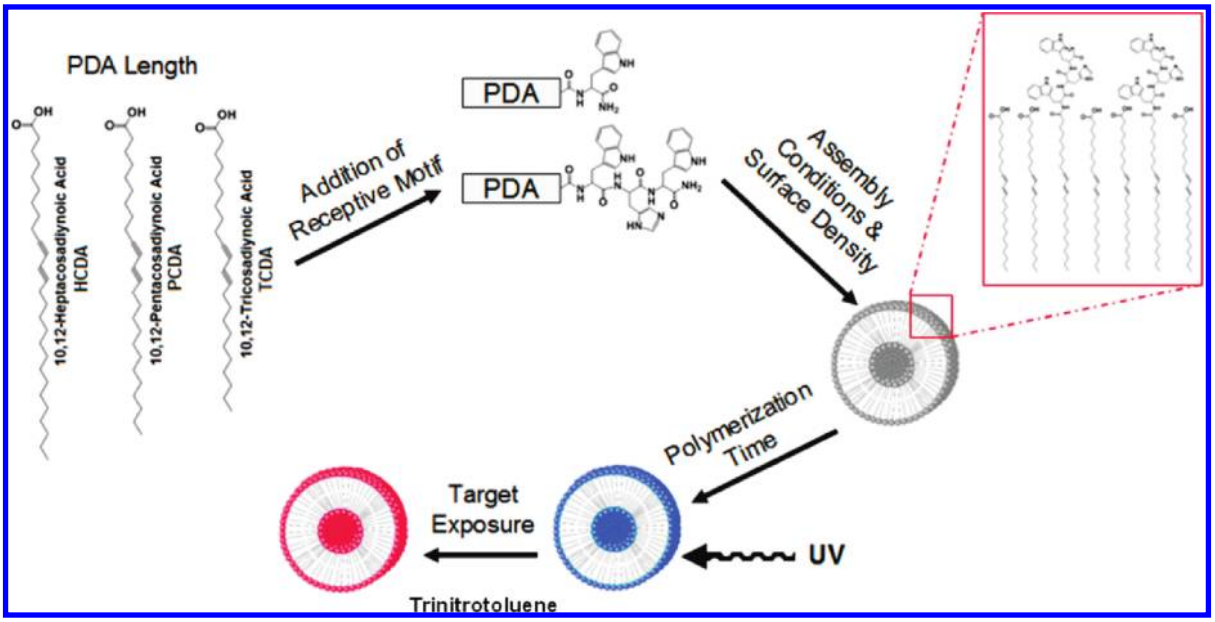

Figure 1. Schematic diagram of the synthesis, composition, and assembly considerations in the design of an effective colorimetric PDA-based sensor for trinitrotoluene.

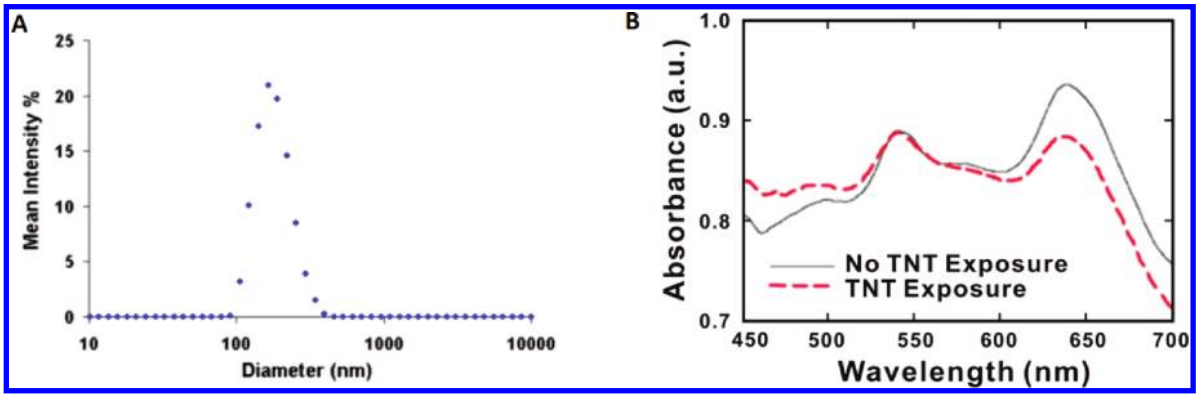

Figure 2. Self-assembled vesicle formation and the vesicles' colorimetric response. (A) Fully polymerized PDA assemblies with a composition of 4% PCDA-Trp-His-Trp and 96% PCDA were used to identify the size of supramolecular assemblies with an average diameter of 162 nm as observed by dynamic light scattering measurements. (B) UV−vis spectra of Trp-His-Trp-PDA/PDA vesicles (4 mol %/96 mol %) in the absence (black solid line) and the presence (red dashed line) of TNT.

solution to the 5 mM PDA-Trp-His-Trp/PDA (4 mol %/96 mol %) suspension resulted in a 2.7% chromic response. As the concentration of TNT increased, the percentage of the chromic response increased, which is in accordance with the concentration dependence of the chromic response previously seen in other PDA-based colorimetric sensors by other research groups.[18,19,26] An analysis of a control suspension of 5 mM PDA-Trp/PDA (4 mol %/96 mol %) with the same 11 μM concentration of TNT provided no chromic response. This chromogenic transition indicated that the association of TNT with PDA-Trp-His-Trp induced changes in the electronic band structures on PDA's conjugated acetylene-vinylene backbone. Therefore, we first analyzed the chemical environment change during TNT target molecule and Trp-His-Trp molecular recognition elements using nuclear magnetic resonance (NMR) spectroscopy. We then characterized this signal transduction event directly by observing changes in UV−vis spectra upon mixing TNT with PDA-Trp-His-Trp assemblies by modulating various parameters, including the chemical composition, receptor density, alkane chain length, and composition.

NMR Studies of Multivalent Interactions with a Tripeptide Receptor (Trp-His-Trp) and TNT. We characterized the multivalent binding interaction between TNT target molecules and the trimer peptide TNT receptor (Trp-His-Trp) using ^{1}H nuclear magnetic resonance (NMR) spectroscopy. We first carried out a binding study to investigate the molecular interactions between TNT and the recognition element. Figure 3a shows the ^{1}H NMR spectra of the aromatic regions of TNT (red line), Trp-His-Trp (green line), and the Trp-His-Trp·TNT complex with a Trp-His-Trp concentration of 9.4 mM and a TNT concentration of 0.57 mM (black line). (For the entire ^{1}H NMR spectra, see Figure S1 in the Supporting Information.) ^{1}H NMR spectroscopy in D_2O revealed upfield shifts of the aromatic proton signals of TNT and the C-2 proton signal of histidine in the mixture of TNT and Trp-His-Trp, compared to the corresponding signals of either TNT or Trp-His-Trp. These chemical shifts indicate the

dx.doi.org/10.1021/la104476p |*Langmuir* XXXX, XXX, 000–000

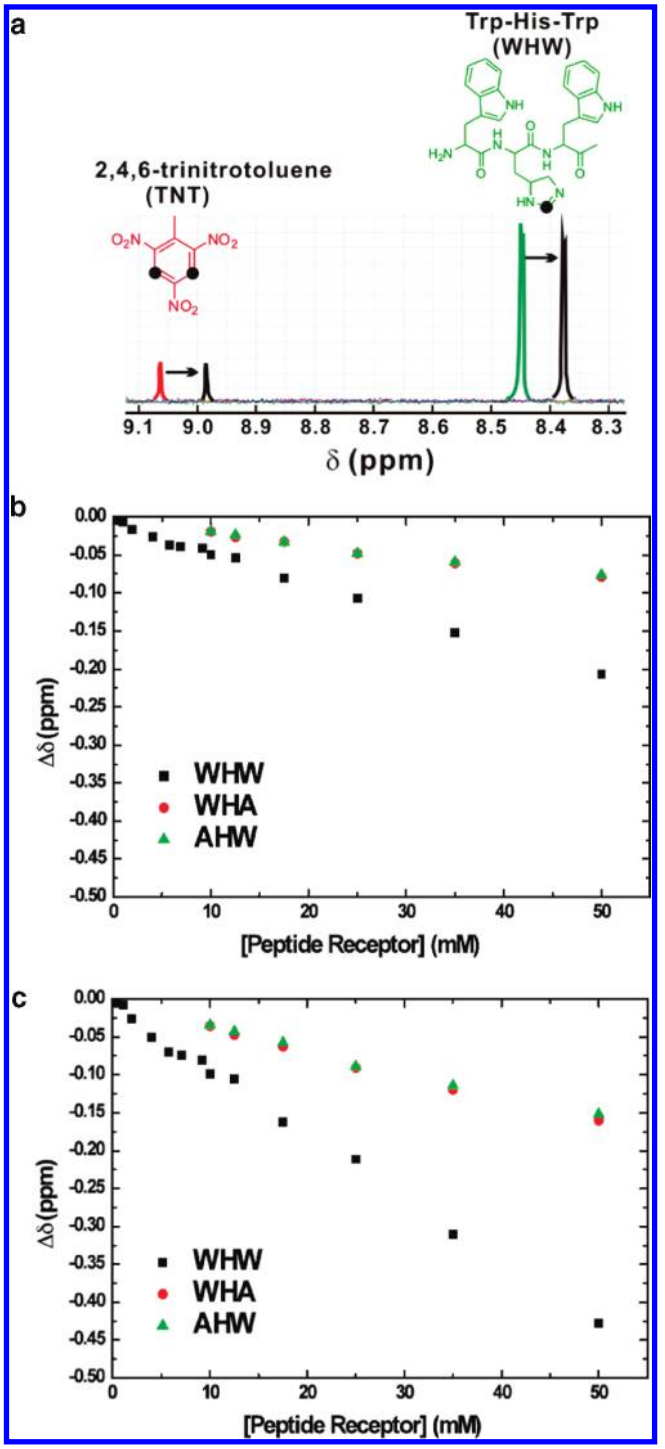

Figure 3. Specific interactions between the receptor (Trp-His-Trp) and TNT. (a) ^{1}H NMR spectra of TNT (red line), Trp-His-Trp (green line), and the (Trp-His-Trp)·TNT complex (black line). (b) Methyl and (c) aromatic protons in TNT exhibiting ^{1}H NMR chemical shift variations, $\Delta\delta$, associated with titrations of 0 to 50 mM concentrations of Trp-His-Trp, Trp-His-Ala, or Ala-His-Trp.

formation of complexes between the receptor (Trp-His-Trp) and TNT. Figure 3b,c shows plots of the variation in chemical shift, $\Delta\delta$, of aromatic and methyl protons on TNT as a function of the receptor concentration in D_2O. Both aromatic and methyl protons on TNT molecules experienced an upfield shift when the receptor (Trp-His-Trp) was added. As the receptor concentration increased, the variation in the chemical shift increased. However, the degree of variation in aromatic protons is higher than that in methyl protons. This indicates that one of the major driving forces of the (Trp-His-Trp)·TNT complex formation is $\pi-\pi$ interactions between tryptophan and TNT's aromatic ring structure. The upfield shift can be explained by the magnetic anisotropy associated with a ring current shielding effect on TNT from the receptor's aromatic rings. Control peptides made by substitutions of the first or third tryptophan to an alanine residue showed a significant reduction in these chemical shifts representing a decreased level of interaction. Thus, we believe that these $\pi-\pi$ interactions of the (Trp-His-Trp)·TNT complex induce the electronic band structure perturbation of Trp-His-Trp-PDA upon binding with TNT target molecules in a multivalent binding manner.

Effects of Polymerization Time on the Maximal Chromic Response. To identify the polymerization time necessary to achieve a sufficiently conjugated backbone (represented by the initial blue color) for sensing purposes, we investigated the relation between the chromic response and UV polymerization of PDA assemblies in our system. Achieving the complete polymerization of assembled PDA is vital in the fabrication of consistent, effective PDA-based sensors. It is this parameter that controls the maximal chromic response that can be achieved for any PDA-based sensor. We characterized the irreversibility of our system and identified the UV exposure necessary for full PDA polymerization. By monitoring the visible absorption spectra at various time intervals after heating and UV exposure, we observed changes in the effective conjugation length (Figure 4a) over the time of exposure. The blue percentage was used to characterize the extent of π-conjugated backbone planarity, where a smaller blue percentage indicates that a larger red phase has been triggered (decreased conjugation). The results seen in Figure 4b demonstrate the pseudoreversibility of the system after heat exposure if the system is insufficiently polymerized. We see that additional UV exposure will create π-conjugated PDA backbones from any previously unpolymerized PDA. The result is a mixture of absorption spectra between previously thermally triggered and newly polymerized PDA. The irreversible nature of the chromatic transition allows a metastable blue phase to enter a more thermodynamically stable red phase upon heating.[38] After several heat and UV cycles (Figure 4b), no change in the π-conjugated backbone can be identified because the blue percentage remains constant after 20 min of total UV exposure. UV polymerization for longer periods of time does not indicate any return to the blue phase. This demonstrates that all available polymerization sites have been reacted. We qualify the polymerization as having reached completion after this 20 min exposure because beyond this timescale the system exhibits its true irreversible nature in terms of chromic response.

To confirm the conditions of complete polymerization and to identify the conditions for maximal chromic response, we analyzed the thermally triggered chromic response of PDA samples after various levels of UV exposure. We observe that the maximal chromic response of 60.2 ± 1.5% is achieved after 20 min (~150 J/cm^2) of 254 nm UV exposure (Figure 4a). Hence, we have identified the minimum UV exposure conditions necessary to polymerize the PDA assemblies fully.

Effects of End-Group Composition. We characterized the effect of end-group size on the ability of PDA sensors to self-assemble effectively. The ability to tune the end-group composition on the side chains is essential to controlling the surface interactions

dx.doi.org/10.1021/la104476p |*Langmuir* XXXX, XXX, 000–000

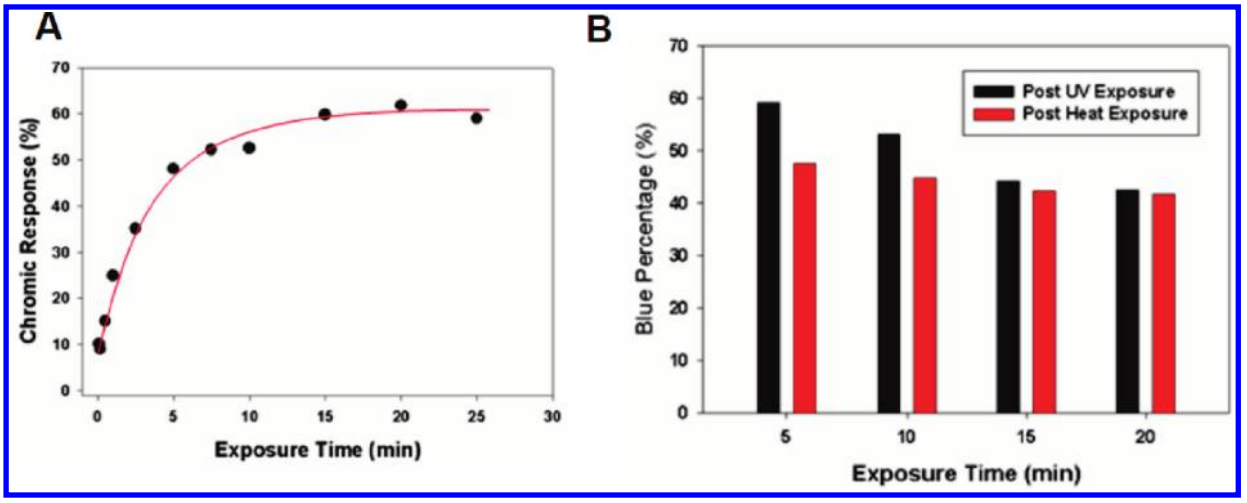

Figure 4. Effect of PDA polymerization times on chromic changes. (A) Varying exposure of PDA assemblies in identifying the conditions for achieving the maximal chromic response (trend line added as a guide) and (B) identifying the length of UV exposure required for full polymerization of the PDA assemblies as indicated by the irreversibility of the system after the repetition of UV and then heat exposure.

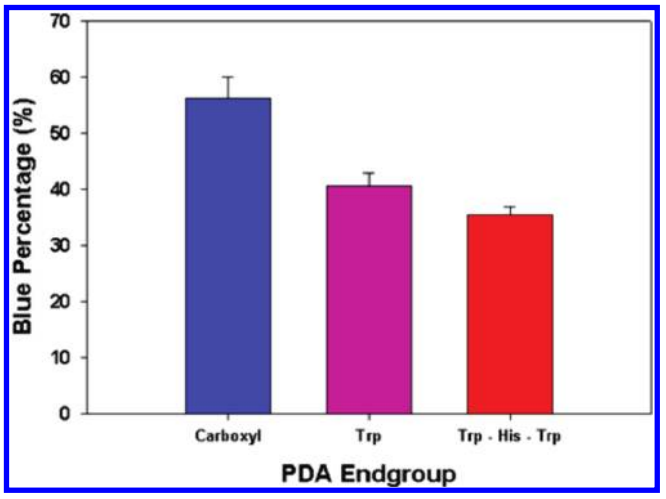

Figure 5. Effect of PDA end-group size. Effect of the PDA functional end group on the initial blue percentage for 100% surface functionality of PCDA (carboxyl), PCDA-Trp, and PCDA-Trp-His-Trp.

experienced by the sensor as well as the extent of monomer alignment in the self-assembly process of the sensor.[47] We functionalized PCDA with trimer peptide receptor Trp-His-Trp. Receptor end groups, such as Trp-His-Trp, are generally bulky components used to interact with particular target molecules of interest in the surrounding environment, which is TNT in this case. The transduction of receptor−target binding into a breaking of backbone planarity is dependent on the side-chain rearrangement.[48,49] Using a 100% surface density of PCDA, PCDA-Trp, and PCDA-Trp-His-Trp, we identified the steric effect of end-group size on the ability of the self-assemblies to retain a planar conjugated backbone. We observe this packing ability by measuring the extent of the initial blue percentage. We see that increasing the steric hindrance through bulkier PDA−peptide conjugates affects the effective packing ability of the PDA side chains, causing a noticeable decrease in the blue percentage (Figure 5). The observed color of PDA is a direct result of the effective conjugation length of the delocalized π-conjugated polymer backbones.[35] Properly aligned monomer side-chain units that undergo UV irradiation will polymerize by means of the reactive diacetylene groups to form blue PDA arrangements that retain their original mesostructure.[50] Aside from stimulus-driven red shifts, misalignment within the PDA assemblies can results in a chromatic transition due to increased HOMO−LUMO spacing of the delocalized π electrons along the PDA backbone. This is directly attributed to the decrease in the effective conjugate length from the reduction in $\pi-\pi$ stacking between adjacent chains.[51,52] With 100% Trp-His-Trp receptor surface density, we see that even prior to the introduction of an external stimulus the sensors will have already reached their red phase, indicating that the conjugation length is insufficient to render any further chromic response. From this, we conclude that high concentrations of bulky receptor end groups sterically restrict the proper alignment of monomer side chains, thereby making such assemblies unusable for sensing purposes. Depending on the target sensing application, it may be essential to use bulky receptors. Therefore, it is important to consider the use of an appropriate surface density to achieve an effective composition of the desired receptor as we explore in the following sections.

Effects of Surface Density. We characterized the surface density of trimer peptide receptors with respect to the chromic response. To maximize the signal transduction, the PDA sensor surface must be incorporated with the appropriate surface density of receptive motifs. We show that a small surface density allows side-chain monomers to pack effectively during self-assembly, thereby ensuring a sufficiently high initial blue percentage that is necessary for signal transduction. Conversely, a high enough density of receptors on the surface is necessary to augment the response to the presence of a target analyte and elicit a change in the adsorption spectra. To investigate this in relation to steric effects, we analyzed the effect of the receptor surface density on the chromic response of the sensor. Because of steric hindrance effects, a 100% surface receptor density prevented proper initial monomer alignment during assembly, causing insufficient conjugation lengths. This caused the pre-exposed self-assemblies to exist in the red phase, which indicates that the sensor was already triggered. To design an effective sensor, it is important to consider this trade-off in the surface density parameter of PDA−peptide conjugates. To analyze this parameter, we observed the blue percentage from the spectra as a function of the Trp-His-Trp receptor surface density in polymerized

dx.doi.org/10.1021/la104476p |*Langmuir* XXXX, XXX, 000–000

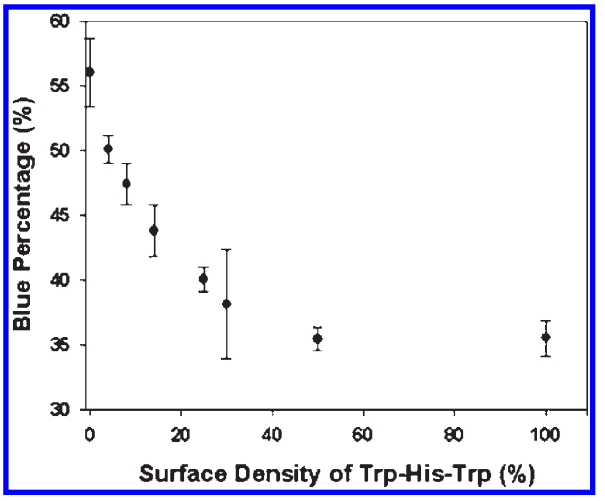

Figure 6. Effect of receptor density on PDA chromic changes. Dependence of initial blue percentage on the surface density of sensors comprising various concentrations of peptide conjugate PCDA-Trp-His-Trp.

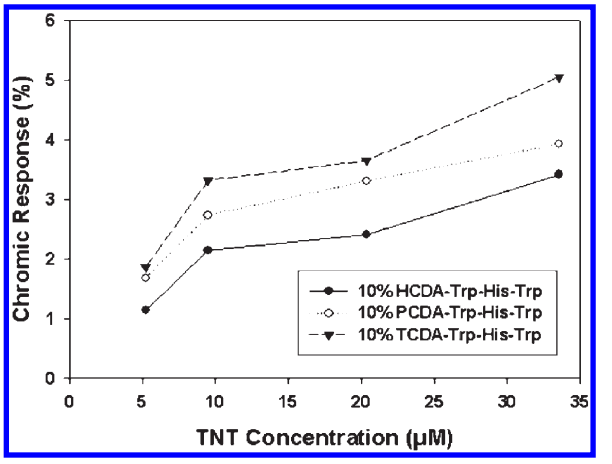

Figure 7. Effect of alkane side-chain length on PDA chromic changes. Dependence of alkane side-chain length on PDA-Trp-His-Trp sensitivity to the TNT target. Decreasing distal alkane lengths facilitate a higher chromic response over a range of TNT concentrations.

sensor assemblies. We can easily identify the extent to which steric hindrance plays a role in breaking the planarity of the conjugated π backbone of PDA (Figure 6). We are particularly interested in identifying this failure point in optical quality in which sterics prevent extended backbone planarity after polymerization. The blue percentage decreases rapidly with increasing surface density such that only assemblies with low Trp-His-Trp surface receptor densities may be considered practical from a sensor perspective. Additionally, we found that the density must be sufficiently high to provide enough transduction sites to disrupt the planar backbone and maximize the chromic response (data not shown). The investigation of this parameter is dependent on the sterics associated with the side-chain functionality and size. Therefore, the fabrication of a PDA sensor must take into account this dependence on the design because the surface density will affect the blue percentage in a surface-receptor-specific manner.

Effects of Alkane Side-Chain Length. We characterized the effects of varying the length of alkane side chains on the PDA backbone in order to enhance the sensor transduction efficacy. The alkane side-chain length of the chromically responsive polymer will play a dramatic role in tuning the chromic response and determining the reversibility of the system. By increasing the chromic response of the system over a range of concentrations, we may effectively amplify the color change for enhanced signal detection. We identified that the alkane side-chain length can influence the sensitivity of the PDA-based sensor, thereby providing a means of increasing the chromic response. Using Trp-His-Trp coupled with shorter or longer alkane side chains (TCDA and HDCA that possess 10- and 14-carbon chains, respectively) than that of PCDA (12-carbon chains, Figure 1), we examined the effect of alkane chain length on the sensitivity of the sensing system to target binding by monitoring the TNT response of HCDA, PCDA, and TCDA conjugates of Trp-His-Trp. As the alkane chain length decreased, we observed an increase in the sensitivity of the systems to the presence of TNT over a range of concentrations (Figure 7). Additionally, we observed a chromic response increase with increasing TNT concentration. A similar chain-length trend has also been observed previously in other PDA-based sensors.[17−19] From our experiments, the largest chromic response to TNT, which was 5.1%, occurred at a TNT concentration of 33.5 μM using 10% TCDA-Trp-His-Trp. Given the large response obtained with the alkane length of TCDA, further analysis was performed using this length of alkane. In particular, the length between the head group and the polydiacetylene backbone was shortened to determine if it may increase the sensitivity of the sensor. The chromic response of 4,6-heptadiynoic acid and 6,8-nonadiynoic acid at a composition of 5% surface density of peptide was found to provide chromic responses of 3.3 and 2.4%, respectively. These levels of chromic response were quite low, indicating that a shorter alkane length between the head group and the backbone does not improve the sensitivity. Conversely, we identified that the alkane chain length from the distal end to the backbone is indeed a critical parameter to be taken into consideration when designing a PDA-based sensing system, where shortening of the alkane distal to the head group conclusively demonstrated a higher sensitivity.

4. CONCLUSIONS

By utilizing a modular synthesis strategy to couple recognition elements to chromically responsive polydiacetylene elements, the essential design parameters for a colorimetric sensor were explored. We provide an in-depth discussion of these system parameters from the aspects of synthesis (receptor and alkane length characteristics), composition (surface density control), and assembly (polymerization considerations). Through UV−vis spectrometry studies, we identified the tripeptide, Trp-His-Trp, as a minimum binding moiety for recognizing TNT molecules and effectively perturbing the conjugated PDA polymer backbone. We further characterized the molecular recognition properties using NMR studies, which provided us with the evidence that Trp-His-Trip could recognize TNT in a multivalent binding mode. With the PCDA-based sensor systems, we also identified the important role of end-group composition, surface density, and alkane side-chain length on the transduction of surface interactions into a chromic response by observing shifts in the absorption spectra. Furthermore, we identified the trade-off that exists in surface density considerations between proper monomer alignment and sufficiently high receptor density to elicit a large chromic response. Although low surface receptor densities can present a potential limitation to these systems in terms of

dx.doi.org/10.1021/la104476p |*Langmuir* XXXX, XXX, 000–000

achieving a large detectable signal, researchers can find consolation in the ability to incorporate these modular PDA−receptor conjugates into carbon nanotube-based field-effect transistors to increase sensitivity dramatically. These results will be useful in the design of colorimetric sensors for other small molecules of interest, and the TNT receptor−PDA conjugate has provided us with a resource for the future development of a sensitive, selective electronic sensor for TNT.

■ ASSOCIATED CONTENT

Supporting Information. NMR spectra of the WHW·TNT complex and further results of polymerized PDA particle characterization by AFM. This material is available free of charge via the Internet at http://pubs.acs.org.

■ AUTHOR INFORMATION

*E-mail: leesw@berkeley.edu.

■ ACKNOWLEDGMENT

Synthesis of the polydiacetylene sensor was supported by the Division of Materials Sciences, which is supported by the Office of Science, Office of Basic Energy Sciences, U.S. Department of Energy, under contract no. DE-AC02-05CH11231. Testing of the sensor chromic response was supported by the Office of Naval Research, the Center of Integrated Nanomechanical Systems (COINS) of the National Science Foundation, and National Science Foundation award no. ECCS-0731309. J.J. also thanks the Bill and Melinda Gates Foundation for support.

■ REFERENCES

(1) Nath, N.; Chilkoti, A. *Anal. Chem.* **2002**, *74*, 504.
(2) Liu, J. W.; Lu, Y. *J. Am. Chem. Soc.* **2003**, *125*, 6642.
(3) Shimada, T.; Ookubo, K.; Komuro, N.; Shimizu, T.; Uehara, N. *Langmuir* **2007**, *23*, 11225.
(4) Chen, S. J.; Huang, Y. F.; Huang, C. C.; Lee, K. H.; Lin, Z. H.; Chang, H. T. *Biosens. Bioelectron.* **2008**, *23*, 1749.
(5) Chah, S.; Hammond, M. R.; Zare, R. N. *Chem. Biol.* **2005**, *12*, 323.
(6) Sugunan, A.; Thanachayanont, C.; Dutta, J.; Hilborn, J. G. *Sci. Technol. Adv. Mater.* **2005**, *6*, 335.
(7) Haes, A. J.; Zou, S. L.; Schatz, G. C.; Van Duyne, R. P. *J. Phys. Chem. B* **2004**, *108*, 6961.
(8) Lucas, L. J.; Chesler, J. N.; Yoon, J. Y. *Biosens. Bioelectron.* **2007**, *23*, 675.
(9) Medintz, I. L.; Clapp, A. R.; Mattoussi, H.; Goldman, E. R.; Fisher, B.; Mauro, J. M. *Nat. Mater.* **2003**, *2*, 630.
(10) Liu, J. W.; Lee, J. H.; Lu, Y. *Anal. Chem.* **2007**, *79*, 4120.
(11) Suman, M.; Freddi, M.; Massera, C.; Ugozzoli, F.; Dalcanale, E. *J. Am. Chem. Soc.* **2003**, *125*, 12068.
(12) Ballester, P.; Shivanyuk, A.; Far, A. R.; Rebek, J. *J. Am. Chem. Soc.* **2002**, *124*, 14014.
(13) Rakow, N. A.; Suslick, K. S. *Nature* **2000**, *406*, 710.
(14) Wang, C. G.; Ma, Z. F. *Anal. Bioanal. Chem.* **2005**, *382*, 1708.
(15) Kolusheva, S.; Kafri, R.; Katz, M.; Jelinek, R. *J. Am. Chem. Soc.* **2001**, *123*, 417.
(16) Su, Y. L.; Li, J. R.; Jiang, L. *Colloids Surf., B* **2004**, *38*, 29.
(17) Biesalski, M.; Tu, R.; Tirrell, M. V. *Langmuir* **2005**, *21*, 5663.
(18) Charych, D. H.; Nagy, J. O.; Spevak, W.; Bednarski, M. D. *Science* **1993**, *261*, 585.
(19) Kim, J. M.; Lee, Y. B.; Yang, D. H.; Lee, J. S.; Lee, G. S.; Ahn, D. J. *J. Am. Chem. Soc.* **2005**, *127*, 17580.
(20) Ma, G. Y.; Cheng, Q. *Langmuir* **2005**, *21*, 6123.
(21) Kolusheva, S.; Shahal, T.; Jelinek, R. *Biochemistry* **2000**, *39*, 15851.
(22) Ahn, D. J.; Kim, J. M. *Acc. Chem. Res.* **2008**, *41*, 805.
(23) Lee, S. W.; Kang, C. D.; Yang, D. H.; Lee, J. S.; Kim, J. M.; Ahn, D. J.; Sim, S. J. *Adv. Funct. Mater.* **2007**, *17*, 2038.
(24) Reppy, M. A.; Pindzola, B. A. *Chem. Commun.* **2007**, 4317.
(25) Song, J.; Cisar, J. S.; Bertozzi, C. R. *J. Am. Chem. Soc.* **2004**, *126*, 8459.
(26) Sukwattanasinitt, M.; Wang, X.; Li, L.; Jiang, X.; Kumar, J.; Tripathy, S. K.; Sandman, D. J. *Chem. Mater.* **1998**, *10*, 27.
(27) Okada, S.; Peng, S.; Spevak, W.; Charych, D. *Acc. Chem. Res.* **1998**, *31*, 229.
(28) Carpick, R. W.; Sasaki, D. Y.; Marcus, M. S.; Eriksson, M. A.; Burns, A. R. *J. Phys.: Condens. Matter* **2004**, *16*, R679.
(29) Kobayashi, A.; Kobayashi, H.; Tokura, Y.; Kanetake, T.; Koda, T. *J. Chem. Phys.* **1987**, *87*, 4962.
(30) Tanaka, H.; Gomez, M. A.; Tonelli, A. E.; Thakur, M. *Macromolecules* **1989**, *22*, 1208.
(31) Lu, Y. F.; Yang, Y.; Sellinger, A.; Lu, M. C.; Huang, J. M.; Fan, H. Y.; Haddad, R.; Lopez, G.; Burns, A. R.; Sasaki, D. Y.; Shelnutt, J.; Brinker, C. J. *Nature* **2001**, *410*, 913.
(32) Jung, Y. K.; Park, H. G.; Kim, J. M. *Biosens. Bioelectron.* **2006**, *21*, 1536.
(33) Ma, G. Y.; Cheng, Q. *Talanta* **2005**, *67*, 514.
(34) Pang, J. B.; Yang, L.; McCaughey, B. F.; Peng, H. S.; Ashbaugh, H. S.; Brinker, C. J.; Lu, Y. F. *J. Phys. Chem. B* **2006**, *110*, 7221.
(35) Tang, Z. H.; Yang, B. A. *J. Mater. Sci.* **2007**, *42*, 10133.
(36) Hoofman, R.; Gelinck, G. H.; Siebbeles, L. D. A.; de Haas, M. P.; Warman, J. M.; Bloor, D. *Macromolecules* **2000**, *33*, 9289.
(37) Burns, A. R.; Carpick, R. W.; Sasaki, D. Y.; Shelnutt, J. A.; Haddad, R. *Tribol. Lett.* **2001**, *10*, 89.
(38) Valenta, C.; Steininger, A.; Auner, B. G. *Eur. J. Pharm. Biopharm.* **2004**, *57*, 329.
(39) Chance, R. R. *Macromolecules* **1980**, *13*, 396.
(40) Huo, Q.; Russell, K. C.; Leblanc, R. M. *Langmuir* **1999**, *15*, 3972.
(41) Jonas, U.; Shah, K.; Norvez, S.; Charych, D. H. *J. Am. Chem. Soc.* **1999**, *121*, 4580.
(42) Kim, J. M.; Lee, J. S.; Lee, J. S.; Woo, S. Y.; Ahn, D. J. *Macromol. Chem. Phys.* **2005**, *206*, 2299.
(43) Cai, M.; Mowery, M. D.; Menzel, H.; Evans, C. E. *Langmuir* **1999**, *15*, 1215.
(44) Jaworski, J. W.; Raorane, D.; Huh, J. H.; Majumdar, A.; Lee, S. W. *Langmuir* **2008**, *24*, 4938.
(45) Grun, J.; Revell, J. D.; Conza, M.; Wennemers, H. *Bioorg. Med. Chem.* **2006**, *14*, 6197.
(46) Kaiser, E.; Colescot, Rl.; Bossinge, Cd.; Cook, P. I. *Anal. Biochem.* **1970**, *34*, 595.
(47) Cheng, Q.; Yamamoto, M.; Stevens, R. C. *Langmuir* **2000**, *16*, 5333.
(48) Song, J.; Cheng, Q.; Zhu, S. M.; Stevens, R. C. *Biomed. Microdev.* **2002**, *4*, 213.
(49) Kew, S. J.; Hall, E. A. H. *Anal. Chem.* **2006**, *78*, 2231.
(50) Peng, H. S.; Tang, J.; Pang, J. B.; Chen, D. Y.; Yang, L.; Ashbaugh, H. S.; Brinker, C. J.; Yang, Z. Z.; Lu, Y. F. *J. Am. Chem. Soc.* **2005**, *127*, 12782.
(51) Li, L. S.; Stupp, S. I. *Macromolecules* **1997**, *30*, 5313.
(52) Lio, A.; Reichert, A.; Ahn, D. J.; Nagy, J. O.; Salmeron, M.; Charych, D. H. *Langmuir* **1997**, *13*, 6524.